

Optical properties of ocular fundus tissues—an *in vitro* study using the double-integrating-sphere technique and inverse Monte Carlo simulation

M Hammer†, A Roggan†, D Schweitzer† and G Müller‡

† Klinikum der Friedrich-Schiller-Universität Jena, Klinik und Poliklinik für Augenkrankheiten, Bachstrasse 18, D-07743 Jena, Germany

‡ Laser-Medizin-Zentrum gGmbH, Kraherstraße 6-10, D-12207 Berlin, Germany

Received 28 July 1994, in final form 25 November 1994

Abstract. Various models have been published calculating the light transport at the ocular fundus either for interpretation of *in vivo* reflectance measurements or for the prediction of photocoagulation effects. All these models took the absorption spectra of the pigments located at the ocular fundus, melanin, haemoglobin, xanthophyll, and the photoreceptor pigments, into account. However, light scattering inside the single fundus layers has not been investigated in detail and was, therefore, neglected in the calculations or only considered by very rough approximations.

This paper presents measurements on specimens of retina, retinal pigment epithelium, choroid, and sclera using the double-integrating-sphere technique. Absorption coefficients, scattering coefficients, and anisotropy of scattering were calculated by an inverse Monte Carlo simulation from the measured collimated and diffuse transmittance and diffuse reflectance. Conclusions are drawn for the interpretation of fundus reflectance measurements, which are a useful tool in diagnostics and photocoagulation dosimetry.

1. Introduction

Compared to other biological tissues, ocular tissues possess very peculiar optical properties (Svaasand and Gomer 1989). This is obvious for the anterior ocular media cornea, aqueous, lens, and vitreous. However, this also holds for the non-transparent posterior part of the eye. While the retinal pigment epithelium and the choroid show a strong absorption over the entire visible wavelength range, the optics of the sclera is predominated by scattering, resulting in its white appearance. The particularity of the neural retina consists in the alignment of the photoreceptors acting as waveguides (Snyder 1975).

The transparency of the anterior eye media allows one to look into the eye and, therefore, enables the ophthalmologist to use light as a tool for diagnostics and therapy. Thus, a more fundamental knowledge of the optical properties of the ocular fundus tissues is necessary to obtain correct applications and interpretations.

In addition to the ophthalmoscopic inspection of the fundus, the spectral analysis of remitted light may be used for the investigation of the metabolism and its pathological alterations in ocular or systemic diseases (Delori and Pflibsen 1989, Kilbride *et al* 1989, Knighton *et al* 1989, van Norren and Tiemeijer 1986, Schweitzer *et al* 1985, 1990, 1992a, b). The interpretation of *in vivo* reflectance spectra requires a model of radiation transfer inside the ocular fundus, as established e.g. by van Norren and Tiemeijer (1986), Delori and Pflibsen (1989), and Schweitzer *et al* (1990). However, checking these models, Hammer

et al (1993) found out that the only model (van Norren and Tiemeijer 1986) fitting their measurements totally neglected scattering effects. Other models, which assumed scattering to appear inside the choroid according to the two-flux theory of Kubelka and Munk (1931) did not fit the measured spectra well. This was not surprising because neither was the illumination of the tissue diffuse nor the scattering inside the tissue isotropic. Thus, the calculation of the actual radiation transfer requires knowledge of not only the absorption spectra of pigments at the ocular fundus but also the scattering parameters of the tissues involved.

In order to fully understand light propagation in biological tissue, the knowledge of its optical properties is indispensable. They are given by scattering caused by inhomogeneities (membranes, nuclei, mitochondria, pigment granules etc) and absorption in constituents (haemoglobin, melanin, NADH, water etc). The corresponding physical parameters are the scattering coefficient μ_s (mm^{-1}) and the absorption coefficient μ_a (mm^{-1}), both depending on the wavelength. For completeness, the scattering phase function $p(s, s')$ describing the probability for a photon to be scattered from a direction s to a direction s' must be known. Within our calculations, the Henyey–Greenstein phase function (Henyey and Greenstein 1941) was applied for the description of a single scattering event. With a certain phase function, the scattering behaviour of tissue can be described by the anisotropy factor g , which is the mean cosine of the scattering angle and which can vary from -1 (backwardly peaked) to $+1$ (forwardly peaked scattering).

Knowing the coefficient and the anisotropy of scattering, it is necessary to estimate how scattering influences the mechanism of thermal tissue damage in photocoagulation. The changes, understood as a rate process of protein denaturation, are described by the damage integral, which is a function of temperature and time. Models of thermal retinal injury developed by Mainster *et al* (1970), Welch and Polhamus (1984), and Birngruber *et al* (1985) analysed the time-dependent temperature profiles by calculation of the heat conduction, assuming light absorption by melanin in the retinal pigment epithelium and the choroid and neglecting scattering. Model calculations taking scattering into account are now available.

2. Material and methods

2.1. Tissue preparation

All measurements were carried out on specimens of native tissue prepared in cuvettes with a diameter of 15 mm and a thickness of 10, 100, or 500 μm . Chemical tissue treatment was excluded as far as possible in order to preserve the native morphology of cellular and subcellular structures, which is responsible for scattering behaviour.

The following layers of the ocular fundus were isolated: neural retina, retinal pigment epithelium, choroid, and sclera. The eyes were obtained from the slaughterhouse, transported in an ice-cooled dewar and prepared within 1–5 h post-mortem.

Bovine eyes were incised about 5 mm posterior to the limbus. After the removal of the anterior part of the eye, the vitreous, and the optic disc, the neural retina was carefully loosened from the eye cup under physiological NaCl solution. The isolated retina was prepared flat into the 500 μm thick cuvette, which was closed by its cover glass. The residual volume was filled with NaCl solution to enable matched boundary conditions and to prevent the retina from drying. For the calculation of the optical parameters, we assumed a retinal thickness of 0.22 mm, given by Prince *et al* (1965). This is in good agreement with the thickness of the human retina, which was given by Rohen (1977) as 0.18 mm at

the equator to 0.23 mm parafoveal. Thus, the bovine retina should be a good model for the human one.

From the porcine eyes, the anterior segment and the vitreous were removed. The eye cups were dissected into four wedge-shaped segments excluding the optic disc. The neural retina was removed. The retinal pigment epithelium (RPE) was carefully scraped from Bruch's membrane under the microscope using a scalpel. Only intact sheets of RPE without attachment of rod outer segments were collected from the solution with a pipette and stored at 0°C. Pigment epithelium of about 10 eyes was used in this preparation. The RPE cell sheets were separated from the solution by centrifugation (5 min at 1000 rpm). The supernatant was discarded and the cell sediment was transferred into the 10 μm cuvette.

The eyes were dissected in the same way for the separation of choroid and sclera. After the removal of the neural retina, the RPE was brushed off with a camel hair brush. Vortex veins were carefully truncated at the inner surface of the sclera and the choroid was removed. We prepared homogenates of choroid and sclera by mortarizing it under liquid nitrogen as Roggan *et al* (1993) have done to fill cuvettes homogeneously with tissue. Homogenized tissues prepared by this procedure showed optical properties that deviated by only a few per cent (1–3%) from those of cut specimens, using a microtome (Peters *et al* 1990). The advantage of the homogenizing technique is the flexible adjustment of different sample thicknesses. However, preliminary examinations by electron microscopy showed that cell membranes and intracellular structures were widely damaged by freezing choroid in liquid nitrogen. Therefore, we used the cryoprotectant solution VS1, first described by Rall and Fahy (1985) and used by Armitage and Rich (1990) for cryopreservation of corneae to achieve vitrification of the tissues. VS1 is a solution of 2.62 mol l⁻¹ dimethylsulphoxide, 2.62 mol l⁻¹ acetamide, 1.32 mol l⁻¹ propane-1,2-diol, and 6% (w/v) polyethylene glycol (average molecular weight 6000 Da) in physiological NaCl solution. The pH of the solution was adjusted to 7.4. After VS1 treatment, the specimens were flattened on an aluminium foil and frozen in liquid propane, cooled in a bath of liquid nitrogen. Freezing in propane was convenient for vitrification because the absence of the Leydenfrost phenomenon led to much higher cooling rates than freezing in liquid nitrogen. The vitrified tissues (choroid and sclera) were pulverized in a mortar and rewarmed in VS1 solution at -20°C. After centrifugation (4000 rpm for 5 min), the supernatant was discarded and the sediment was slowly resuspended by the dropwise adding of physiological NaCl solution. A final centrifugation was carried out before filling the tissue sediment into the cuvettes.

Sclera was taken from five porcine eyes and choroid from about 20 eyes with different melanin pigmentation. Only eyes with totally unpigmented choroids were excluded.

Under *in vivo* conditions, the choroid is like a blood-filled sponge. Immediately after enucleation, the blood was pressed out of the choroid by the intraocular pressure. Therefore, we examined not only the pure choroidal tissue but also mixtures of choroid with native human whole blood. This was taken from the arm vein immediately before the measurement using an EDTA monovette. Unfortunately, the volume fraction of blood in the choroid is unknown. Delori and Pflübsen (1989) estimated it to be approximately 50%. This value agrees with the results of Lorenz *et al* (1988, 1989), who reported that the thickness of histological preparations of the choroid is about one-half of that determined *in vivo* by ultrasonographic measurements. However, Alm (1987) reported a variability of the choroidal blood perfusion of more than 100% in cats, rabbits, and monkeys by nerval-stimulation-induced vasoconstriction and vasodilatation. Considering this variability of blood capacity of the choroid, we examined choroidal tissue mixed with 30%, 50%, and 70% blood content.

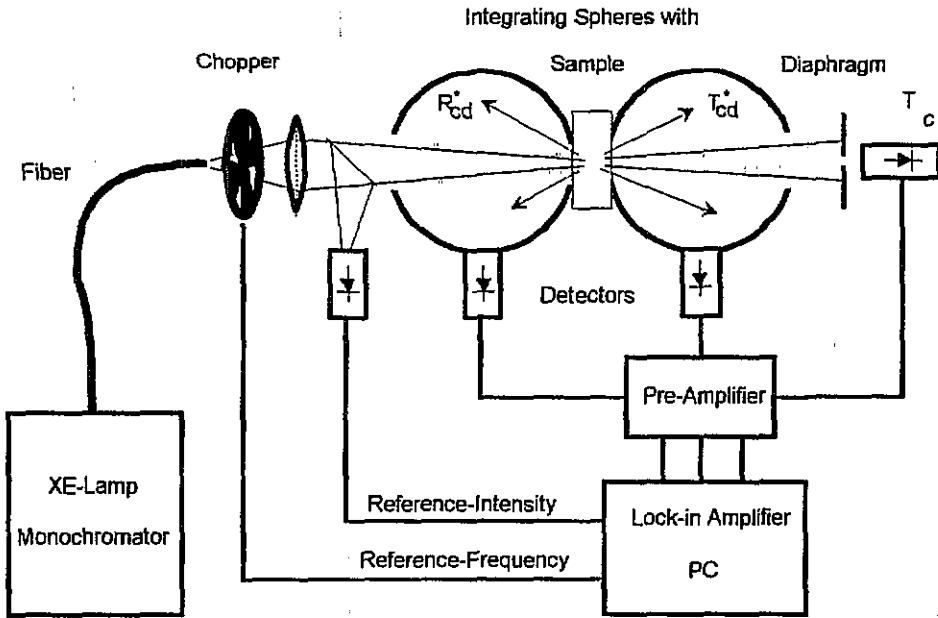


Figure 1. The experimental set-up for the measurements of optical tissue properties.

2.2. Experiment

The measurements were carried out with two integrating spheres (Labsphere Inc., USA; diameter, 30 cm; diameter of sample opening, 12.5 mm; barium oxide coating; $R > 98\%$ in the range 330–1100 nm) and intervening samples prepared as described above (figure 1). The output of a tuneable light source (xenon high-pressure lamp with monochromator, PTI, Germany) was mechanically chopped with 625 Hz and focused on the sample, which was placed inside a quartz cuvette with calibrated thickness (Helma Optik, Germany). The sample diameter was 15 mm, given by the geometry of the cuvettes; the sample thickness was 10 μm for retinal pigment epithelium and 100 μm for choroid and sclera. Since the calculation of the optical constants strongly depends on the sample thickness, we determined its deviations from the calibrated cuvette thickness by measurement using a micrometer screw. For the retina, we adopted a thickness of 220 μm from Prince *et al* (1965; see subsection 3.1). The spot size was approximately 5 mm in diameter and the beam divergence was approximately 1.2°. The slits of the monochromator were adjusted to achieve a FWHM of 10 nm.

At the wavelengths 413, 430, 450, 488, 514, 540, 559, 586, 633, 700, 780, and 1064 nm, the diffuse reflectance R_{cd}^* , the diffuse transmittance T_{cd}^* , and the collimated transmittance T_c were measured by photodiodes SFH 251 (Siemens, Germany, sensitivity, 0.6 A W^{-1} at 850 nm), using the nomenclature of Pickering *et al* (1992). The wavelengths were selected with respect to the extinction maxima of haemoglobin and the emission of lasers used in ophthalmology. The signals were amplified using the lock-in technique and processed by a personal computer. In advance of each measurement, the system was calibrated using a reflectance standard (Labsphere Inc., reflection 99%) and the free light path intensity (for details see Roggan *et al* 1993). The number of measurements was limited to two or three

samples per tissue type due to the expenditure of the inverse Monte Carlo calculation and the complex preparation procedure.

2.3. Calculation of optical tissue parameters

The calculation of the optical tissue properties from experimental data was performed in three steps. Firstly, the measured values R_{cd}^* and T_{cd}^* were corrected for the interaction of both radiation fields inside the integrating spheres, resulting in the values R_{cd} and T_{cd} for diffuse reflection and transmission, respectively. A complete description has been given by Pickering *et al* (1992, 1993) and Roggan *et al* (1993).

Secondly, we calculated the absorption coefficient A and the scattering coefficient S of the Kubelka–Munk theory to obtain a fast approximation for the optical parameters and to obtain initial values for the inverse Monte Carlo simulation:

$$S = (1/(bd)) \ln[(1 - R_{cd}(a - b))/(T_{cd} + T_c)] \quad A = (a - 1)S$$

with

$$a = [1 + R_{cd}^2 - (T_{cd} + T_c)^2]/2R_{cd} \quad b = \sqrt{a^2 - 1}.$$

The corresponding coefficients of the transport theory were derived from the article by van Gemert and Star (1987) as follows:

$$\mu_a = A/2 \quad \mu_s = [(-\ln T_c)/d] - \mu_a \quad g = 1 - (\mu_a + 4S)/3\mu_s.$$

To increase the initial parameter quality, the measured data were corrected for Fresnel reflections at the cuvette boundaries.

The Kubelka–Munk theory can only be applied to diffuse illumination and simple boundary conditions and it is assumed that scattering dominates absorption. Therefore, thirdly, the exact optical properties were calculated with an inverse Monte Carlo simulation by tracing the path of single-photon packages inside the specimen. The pathlength between two interactions was calculated from the mean free pathlength $1/[\mu_a + \mu_s]$ multiplied by the negative logarithm of a random number between zero and one. The photon weight was diminished according to the single-particle albedo at each interaction process. The new photon direction was calculated due to the phase function, applying the redistribution function for the Henyey–Greenstein phase function (Prah 1988). The photon source and the boundary conditions of the Monte Carlo procedure were designed to represent the experimental set-up. This especially concerns the beam divergence, spot size, sample diameter, reflections at glass surfaces, and side losses. According to the statistical nature of Monte Carlo simulations, a sufficient number of photons had to be accumulated to stabilize the results for backward, forward, and collimated intensities. The iterative character of the procedure is caused by the impossibility of giving an explicit expression of the measured intensities from our complex geometry (mismatched boundaries, illumination and detector arrangement, etc) in terms of the optical parameters of the specimen. Thus, there are no forward equations but only forward simulations. Consequently, the inverse problem of extracting optical parameters from measured intensities can be solved only by using a numerical optimizing method.

Starting with the appropriate initial parameters from the Kubelka–Munk equations, a derivation matrix was constructed for the individual intensities. This was done by slightly changing one optical parameter for the corresponding deviation and performing a new

forward Monte Carlo simulation. For each forward calculation, the number of photons was chosen sufficiently high to produce stable results as a necessary presupposition to obtain a smooth plane in the phase space. In this way, the three measured intensities were approached by the conventional gradient method. To reach stable gradients for all parameters, 100 000–500 000 photons had to be generated. This required computation times of up to 4 h per data set on a 486/33 PC. The Monte Carlo calculation was terminated when the differences between measured and simulated data were within 2%. This condition was normally reached after two to five iterations.

For the evaluation of optical thick samples (lack of collimated transmission), a reduced Monte Carlo fit was performed, in which only the two parameters μ_a and μ_s were calculated and g was held fixed. In those cases, the anisotropy was assumed to have the same value as at those wavelengths or sample thicknesses with sufficient intensities at the T_c detector (see discussion).

Reflectance, absorbance, and transmittance for the entire tissue layers and the whole fundus, modelled by their composition, were also calculated from the measured tissue parameters using the Monte Carlo technique (Wang and Jacques 1992). Therefore, specular reflectance was neglected since refractive index differences between the single layers have not been reported for the ocular fundus.

3. Results and discussion

By the described method of the inverse Monte Carlo simulation, we gained the wavelength dependence of the absorption coefficient and the scattering coefficient from measurements of the collimated and diffuse transmission and the diffuse reflection of the specimens. At short wavelengths, the collimated transmission was only a few per cent of the incident radiance or below in all samples. This is due to the large thickness of the retina, the strong absorption of melanin in RPE and choroidal tissue, the absorption of blue and green light by haemoglobin, and the excessive scattering in the sclera. Therefore, we were able to determine the anisotropy of scattering by a three-parameter fit only for longer wavelengths and assumed these values to be valid for the entire wavelength range. This assumption seems to be a good approximation, as can be seen from other tissue measurements in which g varies by only a few per cent from 400 to 1100 nm (van Gemert *et al* 1989, Cheong *et al* 1990, Roggan *et al* 1993).

The reproducibility of the measurements and calculations should be regarded under two aspects. Firstly, errors in the determination of optical parameters were due to the preparation process, the experimental set-up, and the statistical nature of the Monte Carlo simulation. To estimate this error, multiple measurements and calculations were carried out on one tissue type of one individual (human tonsil) in a previous experiment. The tissue was divided into 10 parts, each prepared separately by the homogenizing technique (see 2.1). The homogenizates were measured at 633 nm and the optical parameters were evaluated using the inverse Monte Carlo simulation. The differences for all parameters were within $\pm 2.5\%$ (unpublished data). Secondly, the interindividual variability of optical parameters of the same type of tissue is much larger than the systematic error and depends on individual differences in density, blood content, water content, etc. According to our experience with healthy tissues, the corresponding differences in optical parameters reach up to $\pm 20\%$ for the scattering and the absorption coefficient and up to $\pm 5\%$ for the anisotropy factor. Tumour tissues showed even greater differences, depending on the tumour state (Beuthan *et al* 1994). The specimens of RPE, choroid, and sclera were pooled from several eyes, thus yielding mean values.

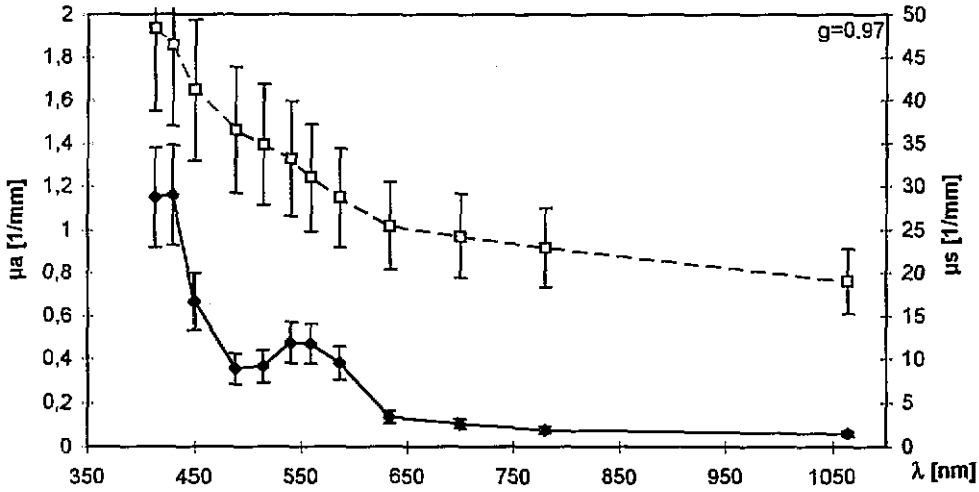


Figure 2. Optical properties of bovine retina, calculated with inverse Monte Carlo simulation.

3.1. The neural retina

The mean absorption and scattering coefficients obtained from two bovine retinæ are shown in figure 2. The anisotropy factor g , determined at 1064 nm, is 0.97. Significant differences within $\pm 20\%$ were observed between the two measured samples. The differences in the absorption are obviously results of different quantities of blood inside the retina. In one of the specimens, a large retinal vessel was centred in the measuring spot, in contrast to the other sample. The differences between the scattering coefficients result from various retinal thicknesses. Their uncertainty is an additional source of errors in the calculation of retinal optical constants.

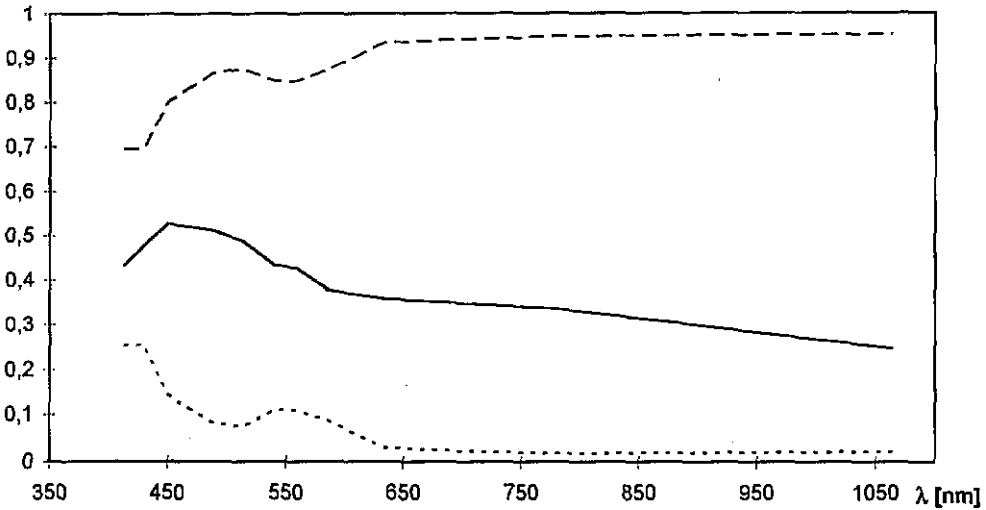


Figure 3. The results of a Monte Carlo simulation for a retina with a thickness of 200 μm : solid line, 10 \times reflection; dotted line, absorption; and broken line, transmission.

From the data of figure 2, the diffuse reflection, total transmission, and absorption of the retina were calculated by Monte Carlo simulation (figure 3). Since the human retinal thickness is given by Rohen (1977) as 100 μm for the fovea, 230 μm for the parafovea, and 180 μm at the equator, we assumed 200 μm for the middle periphery. The calculated transmission between 430 nm and 700 nm was similar to that measured by Pawlowski (1987). Boucher *et al* (1986) measured transmission spectra of isolated bovine retinae identical to ours, except for the rhodopsin peak at 500 nm, which we did not measure, because no attempt was made to prevent bleaching of photosensitive pigments. The calculated reflectance is in good agreement with that measured by Pawlowski (1987) on bovine and human retinae, but, surprisingly, for wavelengths below 633 nm, the reflectance of the isolated retina was calculated to be higher than that of the entire fundus measured *in vivo* (van Norren and Tiemeijer 1986, Delori and Pflibsen 1989, Schweitzer *et al* 1990). In the short-wavelength range, this is due to an additional absorption by the anterior ocular media *in vivo*. Additionally, the higher retinal blood content under *in vivo* conditions may lead to a much higher absorption below 633 nm, resulting in a decreased reflection. On the other hand, van Blokland and van Norren (1986) reported reflectance values of 4% for the temporal retina at 514 nm, which are in the range of our calculations. Moreover, the neural retina is not a homogeneous tissue, but has a well defined structure, which has an influence on the remission of light. Light entering the eye and passing the vitreous is at first partially reflected at the inner limiting membrane. According to Gorrard (1986), the portion of light specularly reflected at this membrane was expected to be one-third of that portion backscattered from the deeper fundus layers (546 nm, 10° temporal). The reflectance of the retinal nerve fibre layer was studied by Knighton *et al* (1989, 1992). They found a reflectance decreasing from about 1.5% at 460 nm to 0.5% at 680 nm, caused by Rayleigh scattering at microtubules and neurofilaments, which are small compared to the wavelength. Further light backscattered from the retina will originate from the inner and the outer nuclear layers. Finally light will be guided by the photoreceptor outer segments, resulting in a directionality of remitted light. Van Blokland and van Norren (1986), therefore, modelled this directional dependence as a superposition of guided and unguided light.

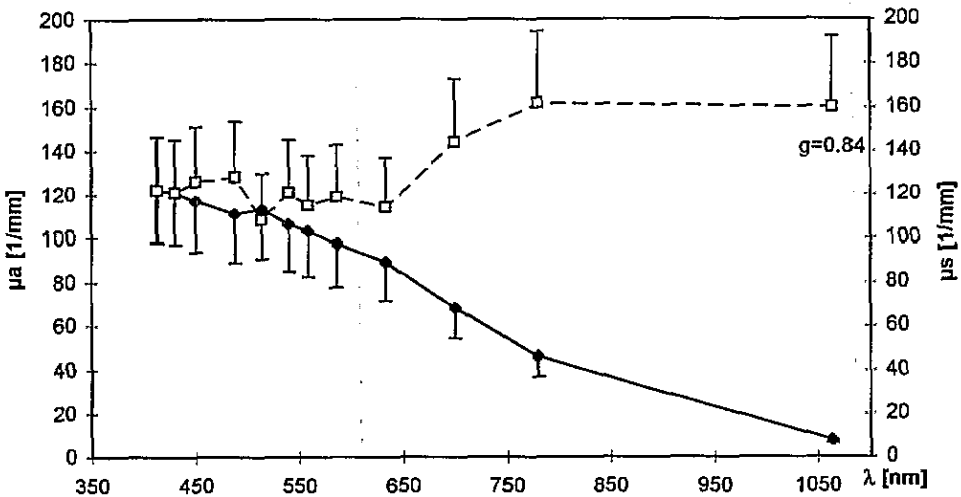


Figure 4. Optical properties of RPE calculated with inverse Monte Carlo simulation.

3.2. The retinal pigment epithelium (RPE)

The optical parameters of RPE cells obtained from measurements at a monocellular layer with a thickness of $10\ \mu\text{m}$ are shown in figure 4. As expected from the dark pigmentation of these cells, in the short-wavelength range the absorption coefficient is nearly as high as the scattering coefficient. The wavelength dependence of absorption is similar to that microspectrophotometrically measured by Gabel *et al* (1978) in glutaraldehyde-fixed sheets of human RPE, though the slope in our measurements was somewhat lower. Scattering takes place at the pigment granules. This was concluded by Bülow (1968) from the interference pattern he observed under the microscope. Thus, the high scattering coefficients we measured corresponded to the density and the size of the retinal pigment granules, which are at $0.5\text{--}1\ \mu\text{m}$ (Ham 1975) about ten times larger than melanin granules in other pigmented human tissues (Drochmans 1966). The slope of the scattering coefficient may be explained by Mie theory, considering the complex refractive index resulting from the strong absorption of the scattering pigment granules.

Reflection, absorption, and transmission of a monocellular layer of RPE cells, which were assumed to be $10\ \mu\text{m}$ thick ($9\text{--}12\ \mu\text{m}$ according to Rohen (1977)), are presented in figure 5. The absorption of the RPE decreased from 75% to 50% between 400 nm and 700 nm. Thus, in spite of its small thickness, the pigment epithelium is the most absorbing tissue in the eye.

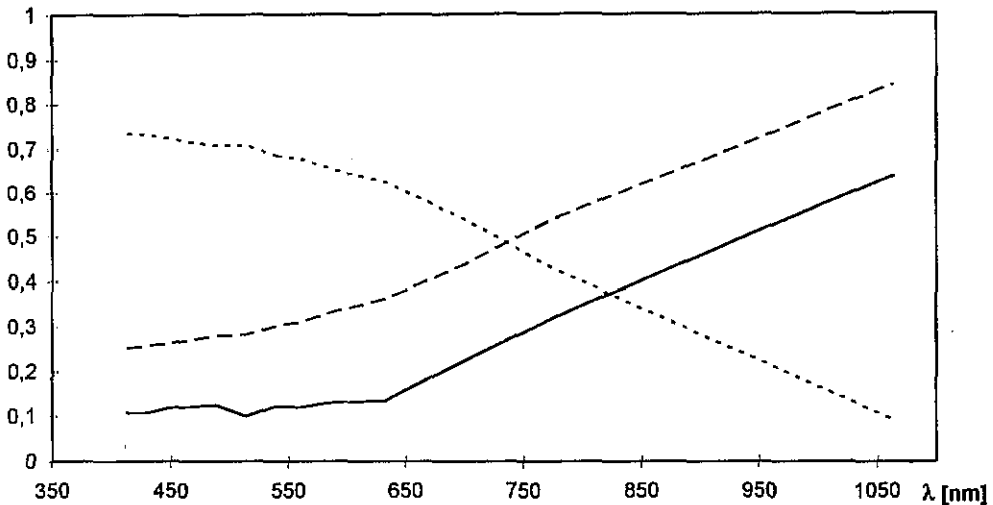


Figure 5. The results of a Monte Carlo simulation for an RPE cell layer with a thickness of $10\ \mu\text{m}$: solid line; $10\times$ reflection; dotted line, absorption; and broken line, transmission.

For interpretation of their *in vivo* reflectance spectra from the human fundus, van Norren and Tiemeijer (1986) introduced an internal reflecting layer. Delori and Pflibsen (1989) concluded from fundus photographs with oblique illumination that the RPE is this reflecting layer. Van Norren and Tiemeijer (1986) and Hammer *et al* (1993) determined the reflectance of this layer from reflectometric measurements to be approximately 1%. This was exactly the reflection of RPE, calculated from our measurements.

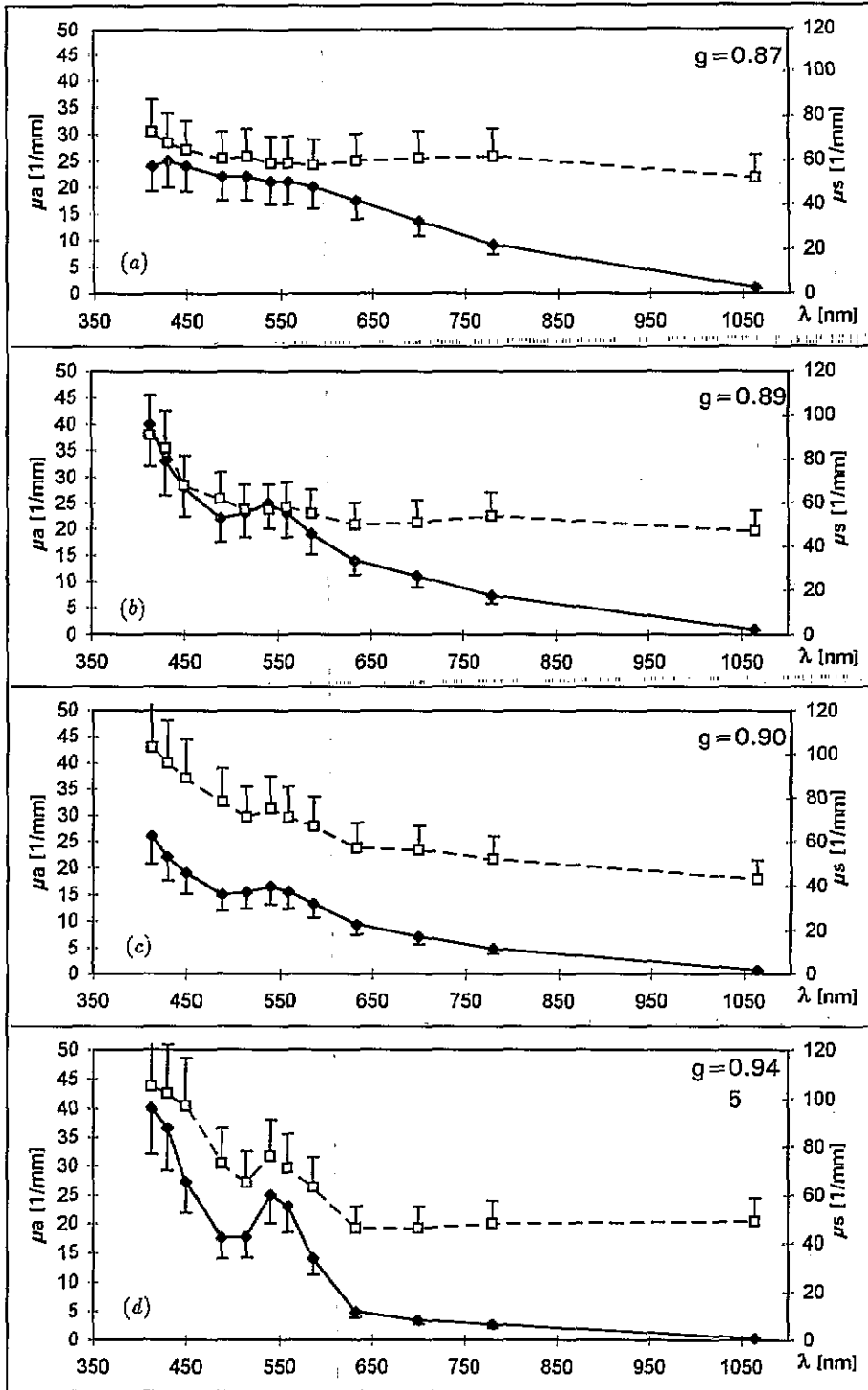


Figure 6. Optical properties of choroid, calculated with inverse Monte Carlo simulation: \blacklozenge — \blacklozenge , μ_a ; \square — \square , μ_s : (a) blood-free specimen; (b)–(d) choroidal tissue, containing 30%, 50%, and 70% whole human blood, respectively.

3.3. The choroid

The calculation of the optical parameters of the choroid proved to be most difficult. The blood-free tissue showed an absorption coefficient determined by melanin absorption, while the scattering coefficient was nearly independent of the wavelength (figure 6(a)). The anisotropy factor determined for choroid at 1064 nm and 780 nm was 0.87. The value increased with increasing blood content of the specimens ($g = 0.945$ at 70% blood portion) due to scattering at the erythrocytes, which were large compared to the wavelength. This agrees with the findings of Reynolds *et al* (1976), who reported $g > 0.99$ for human whole blood for all investigated wavelengths. Unfortunately, the measurements of blood-containing tissue in the 10 μm cuvette were not interpretable by Monte Carlo calculations because this method assumes multiple scattering, which was not given by erythrocytes with a diameter of 8 μm in a layer of 10 μm . Therefore, we calculated our results (figure 6(b)–(d)) from the measurements using cuvettes with a thickness of 100 μm . Consequently, the transmittance of the heavy pigmented choroid mixed with blood was very low and the calculated absorption and scattering coefficients were apparently not independent. However, this disadvantage was compensated within the following calculations because the contribution of both absorption and scattering to the total extinction was considered in the modelling of light transport by forward Monte Carlo simulation (see subsection 3.5).

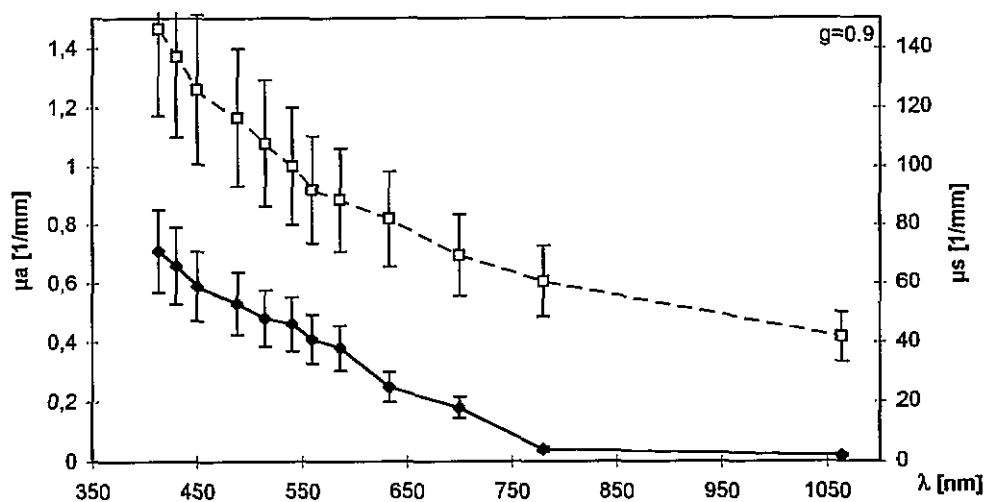


Figure 7. Optical properties of the sclera, calculated with inverse Monte Carlo simulation: \blacklozenge — \blacklozenge , μ_a ; \square — \square , μ_s .

3.4. The sclera

The absorption and scattering coefficients of scleral tissue are shown in figure 7 for an anisotropy factor of $g = 0.9$, determined at 1064 nm. As expected from the white appearance of the sclera, the scattering coefficient greatly exceeds the absorption coefficient. According to Vogel *et al* (1991), this scattering originates from the randomly arranged collagen fibres, which have a mean diameter of 60 nm (Torczynski 1988) and a refractive index of $n = 1.47$ versus $n = 1.36$ for the surroundings (Maurice 1962). The wavelength dependence of the extinction of scleral tissue, which is determined predominantly by

scattering, was found to be proportional to λ^{-3} by Fine *et al* (1985). In contrast, we measured a more even slope of the scattering coefficient, which was proportional to $\lambda^{-1.37}$. From the slope of the absorption coefficient, we assumed absorption to be caused by melanin.

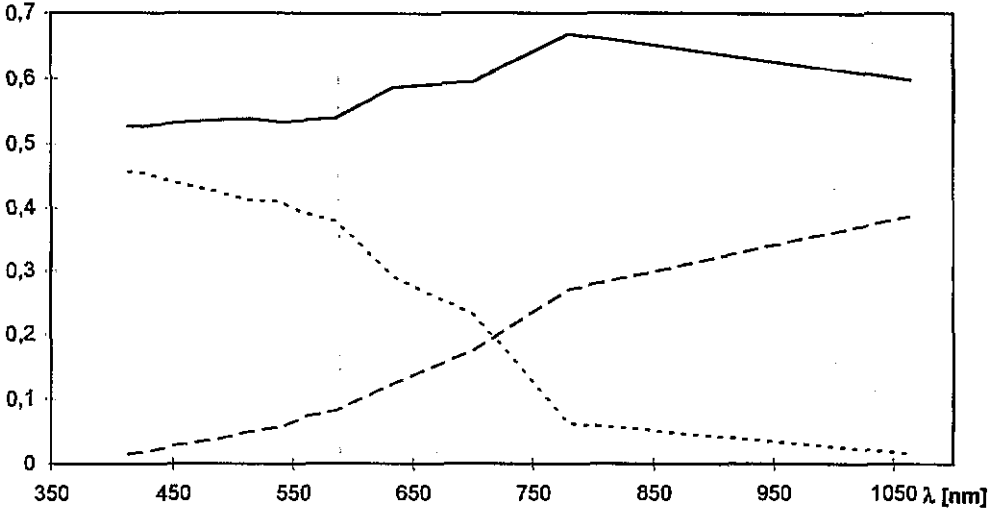


Figure 8. The results of Monte Carlo simulation for a sclera with a thickness of 700 μm : solid line, reflection; dotted line, absorption; and broken line, transmission.

The calculated reflectance, absorption, and transmission (figure 8) for a sclera with a thickness of 0.7 mm (mean value; Rohen 1977) were similar to those measured by Vogel *et al* (1991) for intact human sclera with an integrating sphere. We did not find differences between human and porcine sclera, which they had indicated in their paper. This may be due to the fact that they used tissues from the limbus while we used material from the entire sclera. The pigmentation of the porcine sclera obviously exhibits local differences. While the periphery of the inner surface of porcine sclera appears to be totally white, the posterior pole shows many small pigmented dots.

3.5. Fundus reflectometry

By performing a Monte Carlo simulation of light transport in a layered medium, a fundus reflectance spectrum was modelled. We assumed the fundus structure to be according to Rohen (1977): 200 μm neural retina, 10 μm retinal pigment epithelium, 250 μm choroid, and 700 μm sclera. Thus, the simulation results on the basis of the measured optical tissue coefficients should approximate the *in vivo* fundus reflectance measurements. Figure 9 shows the reflectance spectrum from the fundus temporal to the optic disc of a healthy young male (Hammer *et al* 1993) and the simulated reflectance values, corrected for the double transmission through the anterior ocular media. Optical densities of these media were obtained from the article by van Norren and Vos (1974). The deviation between measured and simulated reflectance in the short-wavelength range is due to stray light inside the fundus reflectometer.

We succeeded in approximating the *in vivo* measurements using the coefficients of the choroidal specimens containing 70% blood. Fundus pigmentation shows a wide

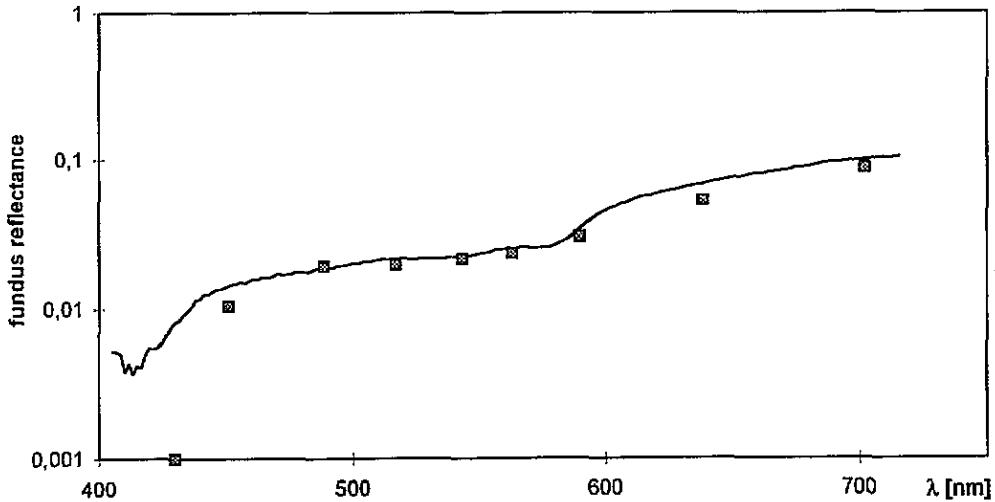


Figure 9. The *in vivo* reflectance spectrum of a human ocular fundus temporal to the optic disc (solid line) and Monte Carlo simulation results for a fundus, composed of 200 μm neural retina (μ_s reduced to 10%), 10 μm RPE (μ_a reduced to 25%), 250 μm choroid containing 70% whole blood, and 700 μm sclera (squares).

interindividual variation, of more than two decades (Delori and Pflibsen 1989). Therefore, the absorption coefficient determined from porcine RPE is not necessarily representative for human RPE. Within our calculation, we had to reduce the measured absorption coefficient to 25% to achieve agreement with the measurement. Furthermore, we had to reduce the scattering coefficient of the neural retina to 10% of the original value. This indicates that the scattering coefficient of the retina obtained from a simple Monte Carlo simulation was overestimated. Thus, the internal structure of the retina and the blood content of this layer have to be taken into account in further investigations.

Generally, Monte Carlo simulations of light transport in the ocular fundus lead to a simple model of fundus reflectance. The advantage compared to the models of van Norren and Tiemeijer (1986), Delori and Pflibsen (1989), and Schweitzer *et al* (1990) is the consideration of anisotropic scattering. Furthermore, the assumption of intermediate reflecting layers is not necessary in this model. The disadvantage is its inconvenience for spectra deconvolution because of the computational expenditure of Monte Carlo simulations.

3.6. Consequences for retinal photocoagulation

The temperature distribution during photocoagulation may be determined by applying the heat conduction equation using the calculated fraction of absorbed light as source term. Therefore, we calculated the absorption versus depth of the applied fundus model by the Monte Carlo method, using the coefficients that fitted the *in vivo* fundus reflectance spectrum at 514 nm (see subsection 3.5). For the sake of comparison, we calculated the absorption for an ocular fundus without scattering according to the Lambert-Beer law. Both absorption profiles are shown in figure 10. Obviously, the absorption per unit volume is the strongest in the retinal pigment epithelium. The absorbance of this layer is predominant. Thus, scattering could be neglected in the extinction of this thin layer. However, the actual temperature distribution has to be calculated with consideration of the lateral broadening

of the laser spot by scattering. Theoretical investigations with consideration of the thermal tissue properties and numerical calculation of the heat conduction are in progress.

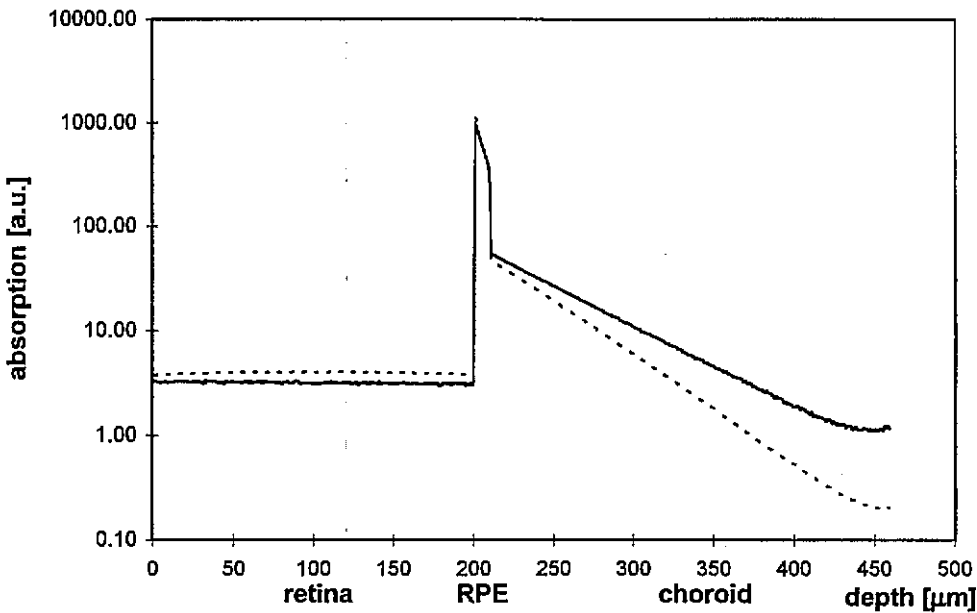


Figure 10. Absorption (arbitrary units) versus fundus depth at $\lambda = 514$ nm: solid line, considering absorption, interrupted and scattering; broken line, considering absorption only.

4. Conclusions

The determination of the absorption, scattering, and anisotropy coefficients of the ocular fundus tissues by the double-integrating-sphere technique is difficult because of the extreme optical properties of these tissues. Despite these difficulties, coefficients were determined that led to the calculation of absorption and transmission spectra of all the fundus layers as well as of the whole fundus. The calculations were in agreement with previously reported *in vivo* and *in vitro* measurements. Only the scattering coefficient of the neural retina seems to have been overestimated. Therefore, further investigations will focus on the mechanism of light transport in this complicated optical structure. The description of fundus reflectance by a Monte Carlo model was successful but further attempts should be made to approximate the reflection by an analytical expression. For an assessment of the importance of scattering for the prediction of photocoagulation, calculations of the temperature profile will be performed in future.

Acknowledgments

We gratefully acknowledge the assistance of Mr Wunderlich and Mr Richter for the cryogenic tissue preparation and of Dr Lemke for the electron microscope examinations of the prepared specimens. This work was supported by grant 01 IN 202 A/4 from the Federal Ministry of Research and Technology of Germany.

References

- Alm A 1987 Der okulären Durchblutung *Okuläre Durchblutungsstörungen* ed R Stodtmeister, T Christ, L E Pillunat and W-D Ullrich (Stuttgart: Enke)
- Armitage W J and Rich S J 1990 Vitrification of organised tissues *Cryobiology* **27** 483-91
- Beuthan J *et al* 1994 Investigations concerning the determination of NADH-concentration using optical biopsy *Lasermedizin* **10** 57-63
- Birngruber R, Hillenkamp F and Gabel V-P 1985 Theoretical investigations of laser thermal retinal injury *Health Phys.* **48** 781-96
- Boucher F, Leblanc R M, Savage S and Beaulieu B 1986 Depth-resolved chromophore analysis of bovine retina and pigment epithelium by photoacoustic spectroscopy *Appl. Opt.* **25** 515-20
- Bülow N 1968 Light scattering by pigment epithelium granules in the human retina *Acta Ophthalmol.* **46** 1048-53
- Cheong W F, Prael S A and Welch A J 1990 A review of the optical properties of biological tissue *IEEE J. Quant. Electron.* **26** 2166-85
- Delori F C and Pflüßsen K P 1989 Spectral reflectance of the human ocular fundus *Appl. Opt.* **28** 1061-77
- Drochmans P 1966 The fine structure of melanin granules *Structure and Control of Melanocytes* ed G Della Porta and O Mühlbock (Berlin: Springer)
- Fine I, Loewinger E, Weinreb A and Weinberger D 1985 Optical properties of the sclera *Phys. Med. Biol.* **30** 565-71
- Gabel V-P, Birngruber R and Hillenkamp F 1978 Visible and near infrared light absorption in pigment epithelium and choroid *Proc. XXIII Consilium Ophthalmologicum (Kyoto, 1978)* ed K Shimizu and J A Osterhuis (Amsterdam: Excerpta Medica)
- Gorrand J-M 1986 Separation of the reflection by the inner limiting membrane *Ophthalmol. Physiol. Opt.* **6** 187-96
- Ham W T 1975 Remarks on fundus reflectance *Vision Res.* **15** 1167-8
- Hammer M, Schweitzer D, Scibor M, Leistritz L and Hoffmann B 1993 Comparison of different models for the radiative transfer to the human ocular fundus using a new technique for spectral reflectance measurement *Proc. 4th Int. Meeting on Scanning Laser Ophthalmoscopy, Tomography and Microscopy (Heidelberg, 1993)* at press
- Heney L G and Greenstein J L 1941 Diffuse radiation in the galaxy *Astrophys. J.* **93** 70-83
- Kilbride P E, Alexander K R, Fishman M and Fishman G A 1989 Human macular pigment assessed by imaging fundus reflectometry *Vision Res.* **29** 663-74
- Knighton R W, Baveze C and Bhattacharya A 1992 The directional reflectance of the retinal nerve fiber layer of the toad *Invest. Ophthalmol. Vis. Sci.* **33** 2603-11
- Knighton R W, Jacobson S G and Kemp C M 1989 The spectral reflectance of the nerve fiber layer of the macaque retina *Invest. Ophthalmol. Vis. Sci.* **30** 2393-402
- Kubelka P and Munk F 1931 Ein Beitrag zur Optik der Farbanstriche *Z. Tech. Opt.* **11** 593-611
- Lorenz B, Birngruber R and Gabel V-P 1988 Experimentelle Untersuchungen zum Verschluss von Aderhautgefäßen durch Infrarotkoagulation im Hinblick auf die Tumortherapie *Fortschr. Ophthalmol.* **85** 726-30
- Lorenz B, Birngruber R and Vogel A 1989 Quantifizierung der Wellenlängenabhängigkeit laserinduzierter Aderhauteffekte *Fortschr. Ophthalmol.* **86** 644-54
- Mainster A W, White T J, Tips J H and Wilson P W 1970 Retinal temperature increase produced by intense light sources *J. Opt. Soc. Am.* **60** 264-70
- Maurice D M 1962 *The cornea and sclera* *The Eye* vol 1, ed H Davson (New York, Academic)
- Pawlowski D 1987 Untersuchungen zum Strahlungstransport im biologischen Gewebe des Augenhintergrundes *Diploma Thesis* Jena
- Peters V G, Wyman D R, Patterson M S and Frank G L 1990 Optical properties of normal and diseased human breast tissues in the visible and near infrared *Phys. Med. Biol.* **35** 1317-34
- Pickering J W, Moes C J M, Sterenborg H J C M, Prael S A and van Gemert M J C 1992 Two integrating spheres with an intervening scattering sample *J. Opt. Soc. Am.* **9** 621-31
- Pickering J W, Prael S A, van Wieringen N, Beek J F, Sterenborg H J C M and van Gemert M J C 1993 Double-integrating-sphere system for measuring the optical properties of tissue *Appl. Opt.* **32** 399-410
- Prael S A 1988 Light transport in tissue *PhD thesis* University of Texas at Austin
- Prince J H, Diesem C D, Eglitis I and Ruskell G L 1965 *Anatomy and Histology of the Eye and Orbit in Domestic Animals* (Springfield, IL: Thomas)
- Rall W F and Fahy G M 1985 Ice-free cryopreservation of mouse embryos at -196°C by vitrification *Nature* **313** 573-5
- Reynolds L, Johnson C and Ishimaru A 1976 Diffuse reflectance from a finite blood medium: applications to the modelling of fiber optic catheters *Appl. Opt.* **15** 2059-67

- Roggan A, Minet O, Schröder C and Müller G 1993 *Measurements of Optical Tissue Properties Using Integrating Sphere Technique (SPIE Institute on Medical Optical Tomography IS 11)* (Washington, DC: SPIE) pp 149-65
- Rohen J W 1977 *Anatomie und Embryologie Augenheilkunde in Klinik und Praxis* ed J Francois and I Hollwich (Stuttgart: Thieme)
- Schweitzer D, Günther S, Scibor M and Hammer M 1992a Spectrometric investigations in ocular hypertension and early stages of primary open angle glaucoma and of low tension glaucoma—multisubstance analysis *Int. Ophthalmol.* **16** 251-57
- Schweitzer D, Klein S, Guenther S, Hammer M and Scibor M 1992b Early diagnosis of glaucoma by means of fundus reflectometry *New Trends Ophthalmol.* **7** 241-7
- Schweitzer D, Königsdörffer E, Tröger G, Augsten R, Klein S and Roth H 1990 Möglichkeiten und Grenzen der Fundusreflektometrie zum Nachweis von Veränderungen in einzelnen Schichten des Augenhintergrundes *Folia Ophthalmol.* **15** 125-37
- Schweitzer D, Schrödel C, Jütte A, Blaschke F and Opfermann F 1985 Spektrometrie am Augenhintergrund—neue diagnostische Möglichkeiten *Folia Ophthalmol.* **10** 299-305
- Snyder A W 1975 Photoreceptor optics—theoretical principles *Photoreceptor Optics* ed A W Snyder and R Menzel (Berlin: Springer)
- Svaasand L O and Gomer C J 1989 *Optics of Tissues (SPIE Institute Series IS 5)* (Washington, DC: SPIE) pp 114-32
- Torcynski E 1988 *Sclera Biomedical Foundations of Ophthalmology* ed T D Duane and E A Jaeger (Philadelphia, PA: Lippincott)
- van Blokland G J and van Norren D 1986 Intensity and polarisation of light scattered at small angles from the human fovea *Vision Res.* **26** 485-94
- van Gemert M J C and Star W M 1987 Relations between the Kubelka-Munk and the transport equation models for anisotropic scattering *Lasers Life Sci.* **1** 287-98
- van Gemert M J C, Jaques S L, Sterenbourg H J C M and Star W M 1989 Skin Optics *IEEE Trans. Biomed. Eng.* **BME-36** 1146-54
- van Norren D and Tiemeijer L F 1986 Spectral reflectance of the human eye *Vision Res.* **26** 313-20
- van Norren D and Vos J J 1974 Spectral transmission of the human ocular media *Vision Res.* **14** 1237-44
- Vogel A, Dlugos C, Nuffer R and Birngruber R 1991 Die optischen Eigenschaften der menschlichen Sklera und deren Bedeutung für transsklerale Laseranwendungen *Fortschr. Ophthalmol.* **88** 754-61
- Wang L-H and Jacques S L 1992 *Monte Carlo Modelling of Light Transport in Multi-layered Tissues in Standard C* The University of Texas, M D Anderson Cancer Center, Houston
- Welch A J and Polhamus G D 1984 Measurement and prediction of thermal injury in the retina of the rhesus monkey *IEEE Trans. Biomed. Eng.* **BME-31** 633-42